

Cite this: *J. Mater. Chem. A*, 2017, 5, 5880

Direct exfoliation of the anode graphite of used Li-ion batteries into few-layer graphene sheets: a green and high yield route to high-quality graphene preparation†

Xifan Chen, Yuanzhi Zhu, Wenchao Peng, Yang Li, Guoliang Zhang, Fengbao Zhang and Xiaobin Fan*

Recycling anode graphite remains a significant barrier to the recovery of used Li-ion batteries. In this study, we show that anode graphite in used lithium-ion batteries is a cheap and ideal candidate for the high yield production of high-quality graphene. Attributed to the reduced interlayer force after repeated charge–discharge cycles, the sonication assisted exfoliation efficiency of the used anode graphite can be 3 to 11 times that of natural graphite, with a highest mass yield of the dispersed graphene sheets of ~40 wt%. Importantly, the layer numbers of most of the exfoliated graphene sheets are 1–4, and their lateral sizes are over 1 μm . Their conductivity after annealing at moderate temperature (500 $^{\circ}\text{C}$) is up to 9100 S m^{-1} , and their potential application in conductive ink was also demonstrated.

Received 14th January 2017
Accepted 21st February 2017

DOI: 10.1039/c7ta00459a

rsc.li/materials-a

Introduction

Several hundred thousand tons of batteries are being produced annually, while the increasing volumes of spent lithium-ion batteries are polluting our environment. Precious metals in these wasted batteries are usually recycled, but recovery of the carbon anode materials of Li-ion batteries has not yet been realized. As the building block of all graphitic forms of carbon materials,¹ graphene has attracted tremendous interest for applications in energy storage devices,² flexible electronics,³ solar cells,⁴ composite fillers,⁵ printed electronics,⁶ heterogeneous catalysis,⁷ etc. Therefore, significant advances have been made in producing graphene over the past decade.^{8–12} For example, Novoselov and Geim first separated a single layer of graphene from highly oriented pyrolytic graphite using the micromechanical exfoliation method,¹³ despite the extremely low yield of this “Scotch Tape Method”. For high yield production, the redox method—usually involving the oxidation of graphite, the exfoliation of the obtained graphite oxide and the reduction/deoxygenation of the graphene oxide—is the most popular method to prepare graphene, especially on an industrial scale. However, residual oxygen functional groups and abundant defects introduced by the oxidation and reduction/deoxygenation processes completely disrupt the ideal sp^2

network and significantly degrade its electronic and mechanical properties. On the other hand, chemical vapor deposition (CVD) is the most promising approach to fabricate graphene with high quality and a large surface area.¹⁴ But the wafer-scale growth of single-crystalline graphene and the complex post-growth transfer process, as well as the high cost remain very great challenges.^{15,16} Alternatively, sonication assisted liquid-phase exfoliation (LPE) of graphite seems to be the best compromise,^{17–20} not only because of the low-defect nature of the obtained graphene, but also due to its easy processability and potentially low cost.

Recently, we found that the pre-intercalation of layered materials like MoS_2 could significantly increase their exfoliation efficiency by LPE. An obvious reduction in the average layer number of the obtained nanosheets was also observed.²¹ We notice that carbon anode materials in used lithium-ion batteries after repeated intercalation may be a cheap and ideal candidate for the high yield production of high-quality graphene by the LPE method (Scheme 1). It may also be an important complement for the recovery of Li-ion batteries. To test this idea, we systematically investigated the direct liquid exfoliation of used anode graphite (UAG) in both an aqueous surfactant solution and a solvent mixture.

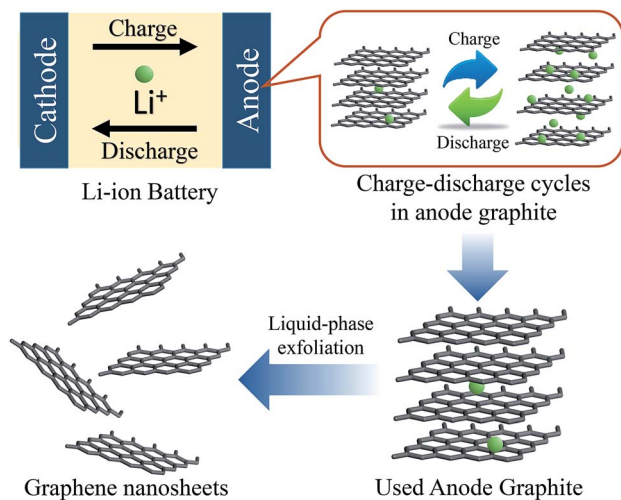
Experimental methods

Materials

Wasted Li-ion batteries were purchased with product number HB6A2L (Huawei), sodium cholate (SC) was purchased from Tokyo Chemical Industry Co. Ltd (product number S0596), and graphite flakes were purchased from Sigma-Aldrich (product

School of Chemical Engineering and Technology, State Key Laboratory of Chemical Engineering, Collaborative Innovation Center of Chemical Science and Engineering, Tianjin University, Tianjin 300072, People's Republic of China. E-mail: xiaobinfan@tju.edu.cn

† Electronic supplementary information (ESI) available. See DOI: 10.1039/c7ta00459a



Scheme 1 Illustration of the preparation of graphene with used anode graphite by liquid-phase exfoliation.

number 282863). Glycerol, ethylene glycol and absolute ethyl alcohol were purchased from Tianjin Guangfu Chemical Co. Ltd.

Preparation

The used anode graphite (UAG) powder in this experiment was obtained from wasted Li-ion batteries, which was then rinsed with deionized water and dried for 24 h in a vacuum oven at 60 °C. Dispersions were prepared by adding UAG powder or graphite powder (2 mg mL⁻¹) to 15 mL aqueous surfactant solution (6 mM SC), which is a modified method reported previously.²² The samples were exfoliated by horn sonication (QSONICA, Q700) for 2 h (15% × 700 W) at ~5 °C. After sonication, the dispersions were centrifuged at 1000 rpm (Sigma 3–18 K) for 40 min, and the top 10 mL was carefully collected and then washed three times with deionized water. The mass yields were obtained by a vacuum drying method.²¹

Thin free-standing films were fabricated by vacuum filtration. Then, the films were thermally annealed at 500 °C to remove any residual sodium cholate for further characterization. To prepare conductive ink, the as-made graphene sheets were dispersed in an ethanol–ethylene glycol–glycerol (50 : 45 : 5 vol%) mixed solution (10 mg mL⁻¹).²³

Characterization

The samples were characterized by transmission electron microscopy (TEM, JEM-2100F, JEOL), scanning electron microscopy (SEM, S-4800, HITACHI), Atomic Force Microscopy (AFM, CSPM5500, BENYUAN), X-ray photoelectron spectroscopy (PHI5000 Versa Probe), Raman spectroscopy (Renishaw inVia reflex), X-ray diffraction (XRD, D8-Focus, Bruker Axs), UV-vis-NIR spectrophotometry (3802 UNIC), and a four-point probe method (RST-9 4 PROBES TECH).

Results and discussion

The used anode graphite (UAG) powder obtained from wasted Li-ion batteries was washed with water for purification and then

vacuum dried for further use. X-ray diffraction (XRD) analysis confirms that the UAG shows an identical pattern to natural graphite, despite its relatively lower intensity (Fig. 1). Compared with natural graphite, however, the normalized (002) peak of UAG shows an obvious shift to a lower angle (inset), indicating the slight increase of the interlayer distance. The interlayer distances of the UAG and graphite powders have been calculated from the Bragg equation to be 0.338 and 0.335 nm, respectively. Note that an increase in the interlayer distance of van der Waals crystals suggests a reduction in interlayer force and facilitates the subsequent exfoliation process.²⁴

To compare the exfoliation efficiency, bulk UAG or natural graphite was first exfoliated by probe sonication in aqueous 6 mM sodium cholate solution,^{22,25} an effective system to exfoliate layered van der Waals crystals. We found that the concentration of the UAG-made graphene dispersion after centrifugation (1000 rpm for 40 min, optimized by UV-vis and AFM analyses Fig. S1†) was much higher than that of graphite, and the difference could be clearly recognized by the naked eye, especially in the diluted dispersions as shown in Fig. 2a. More images of graphene sheets are shown in Fig. S2.† Note that this concentration difference is further enlarged when exfoliated in a 45 vol% ethanol–water solution (10 times difference in concentration, see more details in Fig. S3†),^{26,27} but a significant decrease in concentration was observed in both the UAG- and graphite-made dispersions. The UV-vis absorption spectra (Fig. 2b) reveal that the absorption peak of both UAG and graphite dispersions appears at ~268 nm, indicating that the electronic conjugation within the graphene sheets is retained.²⁸ Notably, the concentration of the UAG-made graphene dispersion was measured to be ~0.8 mg mL⁻¹ by vacuum drying methods, corresponding to a mass yield of ~40 wt% (statistical data of 10 times). This value is 3 times that of the graphite-made dispersion and much higher than the reported results.^{18,22,29}

TEM analysis was employed to examine the thickness and the quality of the graphene sheets. Typical transparent graphene sheets with lateral dimensions over 1 μm in the UAG-made dispersion are represented in Fig. 3a. The bilayer structure and

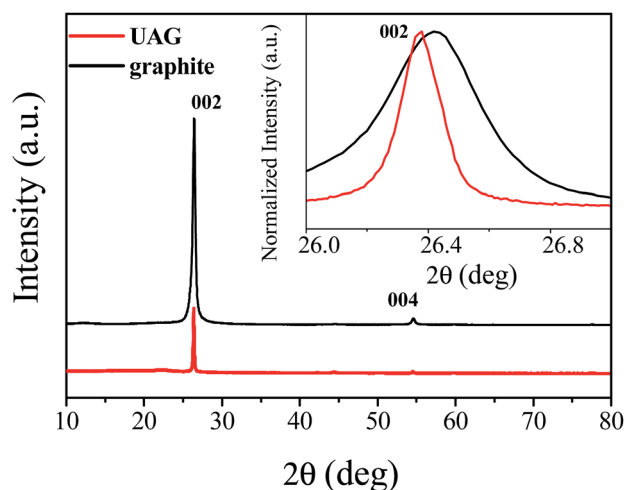


Fig. 1 XRD patterns of UAG (red line) and graphite (black line).

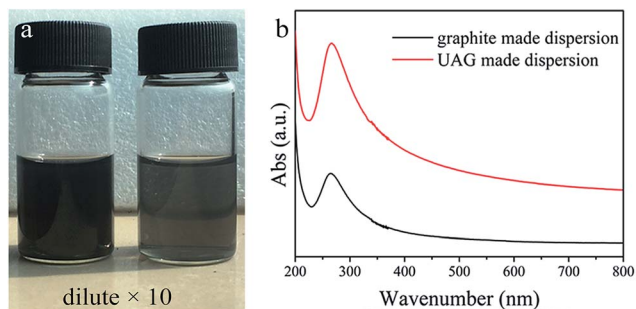


Fig. 2 (a) Digital images of the UAG-made dispersion (left) and graphite-made dispersion (right). The dispersions were diluted 10-fold for comparison. (b) UV-vis spectra of graphite (black line) and UAG (red line). The initial graphite or UAG concentration was 2 mg mL^{-1} , and sonication ($15\% \times 700 \text{ W}$) was carried out for 2 h followed by standard centrifugation at 1000 rpm for 40 min.

further opening on the edges can be directly observed under HRTEM (Fig. 3b). Despite the presence of adsorbed sodium cholate which is impossible to be completely removed,²² the hexagonal lattice is vivid in the Fourier transform images (Fig. 3a,

inset). The high-quality nature of the obtained graphene was further supported by the hexagonal pattern of selected area electron diffraction (SAED). Interestingly, AFM analysis (Fig. 3c) reveals a large number of graphene flakes with clear steps after sonication for 1 h. In line with previous studies,³⁰ the apparent AFM thickness of the first step is always larger than that of the second one (Fig. S4†), which is likely caused by the instrumental offset arising from different interaction forces between the AFM probe, the graphene, and the substrate.³¹ Further exfoliation was achieved by prolonged sonication (2 h) and abundant nanosheets with a thickness of $\sim 1.5 \text{ nm}$ and lateral size over $1 \mu\text{m}$ were observed (Fig. 3e). The lateral size and height distribution based on 71 sheets are showed in the histogram, and 45 sheets had sizes over $1 \mu\text{m}$ and thicknesses less than 1.5 nm (Fig. 3f and g). The majority of the graphene sheets had a lateral size of $1\text{--}3 \mu\text{m}$ and a thickness of less than 3 nm . Considering the adsorbed sodium cholate³² and the intrinsic ripples in graphene,³³ the layer numbers of the exfoliated graphene in the final dispersion were estimated to be 1–4.

Raman spectroscopy was also used to quantify the defects. As shown in Fig. 4, the Raman spectrum of the starting UAG is characterized by a defect induced D-band (1337 cm^{-1}), a G-band

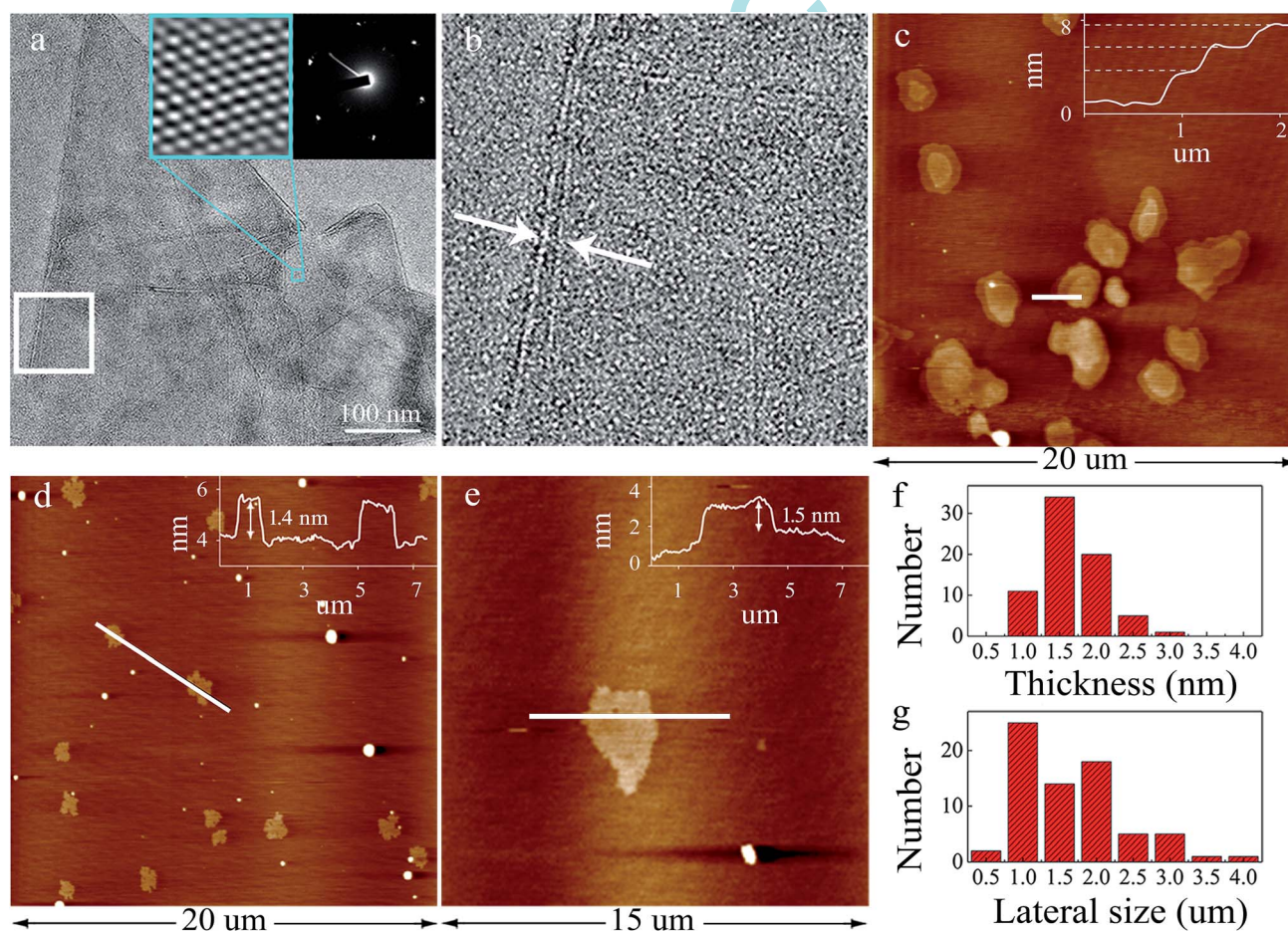


Fig. 3 (a) Typical TEM image of the obtained graphene sheets. (b) Enlarged image on the edge (the white square in a). (c) Typical AFM images of the graphene flakes with clear open steps after sonication for 1 h. (d and e) AFM images of the obtained graphene sheets after prolonged sonication (2 h). (f) Thickness distribution and (g) lateral size distribution were counted from 71 nanosheets. UAG was sonicated ($15\% \times 700 \text{ W}$) for (c) 1 h or (a, b and d–g) 2 h followed by standard centrifugation at 1000 rpm for 40 min.

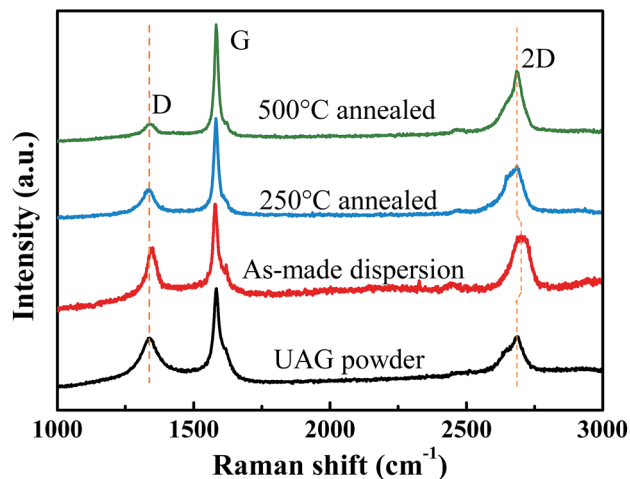


Fig. 4 Raman spectra of UAG and representative as-made graphene with different treatments. The excitation wavelength was 633 nm.

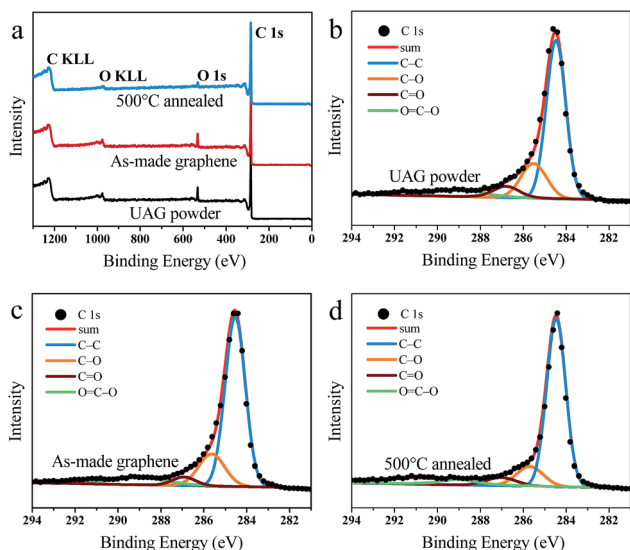


Fig. 5 (a) XPS survey and (b–d) high-resolution C1s spectra of (b) UAG, (c) graphene film and (d) graphene film annealed at 500 °C.

(1583 cm^{-1}), and a 2D-band (2684 cm^{-1}). We can quantify the defect level by the intensity ratio of D-band to G-band, I_D/I_G .⁹ The I_D/I_G of 0.54 for UAG is obviously higher than that of

pristine graphite, suggesting that some defects were introduced after repeated charge–discharge cycles in the dead batteries. However, the I_D/I_G value increased only slightly to 0.68 after exfoliation, due to the increase of defects and edges. However, this value is still much lower than that of chemically reduced graphene³⁴ and is comparable to those of the graphene sheets exfoliated by LPE.^{35–38} Notably, after annealing at moderate temperatures, the ratio of I_D/I_G can be significantly reduced to 0.33 (annealing at 250 °C) and 0.14 (annealing at 500 °C). In addition, it has long been known that the shape of the 2D-band indicates the number of layers in the graphene sheets.³⁹ Compared to that of the UAG powder, the 2D band of the exfoliated dispersion became symmetrical and sharp in shape, meaning that the graphene nanosheets are of <5 layers,^{9,39} in good agreement with the AFM and TEM data. The blue shift of the 2D band may be caused by the local strain introduced by the adsorbed surfactant. On the other hand, an obvious change in shape and red-shift of the 2D band are readily observed in the deposited films after annealing, indicating the restacking of graphene sheets.^{22,37,40}

Further characterizations were carried out by using XPS. As shown in Fig. 5a, the oxygen percentage in UAG powder is estimated to be 7%, whereas the oxygen contents of the exfoliated graphene and the deposited film after annealing (500 °C) are 9% and 3%, respectively. The corresponding high-resolution C1s spectra (Fig. 5b–d) are dominated by a feature at around 284.5 eV, which represented the graphitic carbon. In addition, fitting procedures show three small peaks corresponding to carbon bonds (C–O) at 285.6 eV, (C=O) at 287 eV, and (O=C–O) at 289 eV, respectively. The similar spectra of UAG and exfoliated graphene (Fig. 5b and c) suggest that only a few functionalities were introduced during the sonication process. Besides, these functional groups can be readily reduced after moderate annealing treatment, in accordance with the Raman results.

To measure the conductivity of the exfoliated graphene, a free-standing film with a thickness of $\sim 50 \mu\text{m}$ was prepared by vacuum filtration (Fig. 6a). Different from the graphene oxide paper or reduced graphene oxide films that show a well-packed layer structure,⁴¹ the cross-sectional SEM image of our sample shows random restacking of few-layer graphene sheets with good stiffness (Fig. 6b). After annealing at 500 °C, the

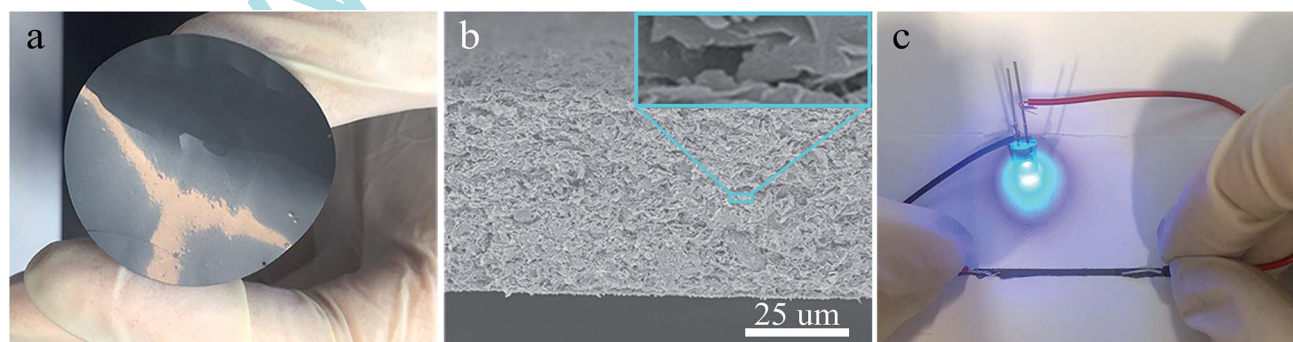


Fig. 6 (a) Digital image of a free-standing film. (b) Cross-sectional SEM image of the film in (a). (c) Digital image of the electrical circuit drawn using a rollerball pen on common paper.

direct-current (DC) conductivity of the graphene film can reach 9100 S m^{-1} . This electrical conductivity is quite high compared with previous studies,^{42–45} while the corresponding value for the UAG powder is only 4500 S m^{-1} . To evaluate the potential application of the exfoliated graphene sheets in conductive ink, the as-made graphene sheets were dispersed in an ethanol–ethylene glycol–glycerol (50 : 45 : 5 vol%) mixed solution at a concentration of 10 mg mL^{-1} (Fig. S5†). As illustrated in Fig. 6c, a conductive track was drawn using a rollerball pen on common paper, and a light-emitting diode (LED) could work normally when the conductive track was connected to an electrical circuit. Note that a lower concentration cannot guarantee the complete covering of the track by graphene sheets after drying. This result suggests that the as-made graphene sheets here can be applied in flexible conductive patterns with high conductivity on paper substrates.

Conclusion

In conclusion, we report a new strategy for recycling used anode graphite to prepare graphene sheets by sonication assisted liquid-phase exfoliation. We found that the exfoliation efficiency of the used anode graphite was increased by 3 to 11 times relative to natural graphite, with a highest mass yield of ~40 wt%. We revealed that more than 60% of the as-made graphene flakes had sizes over $1 \mu\text{m}$ and thicknesses less than 1.5 nm. Besides, their conductivity can reach 9100 S m^{-1} , and their application in conductive ink was also demonstrated. More importantly, this technique in combination with the precious metal recycling process may result in an environment friendly, high-efficiency and high value-added recycling technology for used batteries.

Acknowledgements

This study is supported by the National Natural Science Funds (No. 21676198) and the Program of Introducing Talents of Discipline to Universities (No. B06006).

Notes and references

- 1 A. K. Geim and K. S. Novoselov, *Nat. Mater.*, 2007, **6**, 183–191.
- 2 F. Bonaccorso, L. Colombo, G. Yu, M. Stoller, V. Tozzini, A. C. Ferrari, R. S. Ruoff and V. Pellegrini, *Science*, 2015, **347**, 1246501.
- 3 L. Kou, T. Huang, B. Zheng, Y. Han, X. Zhao, K. Gopalsamy, H. Sun and C. Gao, *Nat. Commun.*, 2014, **5**, 3754.
- 4 J. T. W. Wang, J. M. Ball, E. M. Barea, A. Abate, J. A. Alexander-Webber, J. Huang, M. Saliba, I. Mora-Sero, J. Bisquert, H. J. Snaith and R. J. Nicholas, *Nano Lett.*, 2014, **14**, 724–730.
- 5 G. Mittal, V. Dhand, K. Y. Rhee, S.-J. Park and W. R. Lee, *J. Ind. Eng. Chem.*, 2015, **21**, 11–25.
- 6 A. E. Jakus, E. B. Secor, A. L. Rutz, S. W. Jordan, M. C. Hersam and R. N. Shah, *ACS Nano*, 2015, **9**, 4636–4648.
- 7 A. Zitolo, V. Goellner, V. Armel, M. T. Sougrati, T. Mineva, L. Stievano, E. Fonda and F. Jaouen, *Nat. Mater.*, 2015, **14**, 937–942.
- 8 K. S. Kim, Y. Zhao, H. Jang, S. Y. Lee, J. M. Kim, K. S. Kim, J. H. Ahn, P. Kim, J. Y. Choi and B. H. Hong, *Nature*, 2009, **457**, 706–710.
- 9 K. R. Paton, E. Varrla, C. Backes, R. J. Smith, U. Khan, A. O'Neill, C. Boland, M. Lotya, O. M. Istrate, P. King, T. Higgins, S. Barwich, P. May, P. Puczkarski, I. Ahmed, M. Moebius, H. Pettersson, E. Long, J. Coelho, S. E. O'Brien, E. K. McGuire, B. M. Sanchez, G. S. Duesberg, N. McEvoy, T. J. Pennycook, C. Downing, A. Crossley, V. Nicolosi and J. N. Coleman, *Nat. Mater.*, 2014, **13**, 624–630.
- 10 D. Voiry, J. Yang, J. Kupferberg, R. Fullon, C. Lee, H. Y. Jeong, H. S. Shin and M. Chhowalla, *Science*, 2016, **353**, 1413–1416.
- 11 X. Xu, Z. Zhang, L. Qiu, J. Zhuang, L. Zhang, H. Wang, C. Liao, H. Song, R. Qiao, P. Gao, Z. Hu, L. Liao, Z. Liao, D. Yu, E. Wang, F. Ding, H. Peng and K. Liu, *Nat. Nanotechnol.*, 2016, **11**, 930–935.
- 12 K. Parvez, Z.-S. Wu, R. Li, X. Liu, R. Graf, X. Feng and K. Muellen, *J. Am. Chem. Soc.*, 2014, **136**, 6083–6091.
- 13 K. S. Novoselov, A. K. Geim, S. V. Morozov, D. Jiang, Y. Zhang, S. V. Dubonos, I. V. Grigorieva and A. A. Firsov, *Science*, 2004, **306**, 666–669.
- 14 X. Zhang, J. Xin and F. Ding, *Nanoscale*, 2013, **5**, 2556–2569.
- 15 A. V. Zaretski and D. J. Lipomi, *Nanoscale*, 2015, **7**, 9963–9969.
- 16 L. Gao, G. X. Ni, Y. Liu, B. Liu, A. H. Castro Neto and K. P. Loh, *Nature*, 2014, **505**, 190–194.
- 17 Y. Hernandez, V. Nicolosi, M. Lotya, F. M. Blighe, Z. Sun, S. De, I. T. McGovern, B. Holland, M. Byrne, Y. K. Gun'Ko, J. J. Boland, P. Niraj, G. Duesberg, S. Krishnamurthy, R. Goodhue, J. Hutchison, V. Scardaci, A. C. Ferrari and J. N. Coleman, *Nat. Nanotechnol.*, 2008, **3**, 563–568.
- 18 C. Yeon, S. J. Yun, K.-S. Lee and J. W. Lim, *Carbon*, 2015, **83**, 136–143.
- 19 T. Q. Lin, J. Chen, H. Bi, D. Y. Wan, F. Q. Huang, X. M. Xie and M. H. Jiang, *J. Mater. Chem. A*, 2013, **1**, 500–504.
- 20 Y. C. Yang, F. Lu, Z. Zhou, W. X. Song, Q. Y. Chen and X. B. Ji, *Electrochim. Acta*, 2013, **113**, 9–16.
- 21 X. Fan, P. Xu, Y. C. Li, D. Zhou, Y. Sun, M. A. Nguyen, M. Terrones and T. E. Mallouk, *J. Am. Chem. Soc.*, 2016, **138**, 5143–5149.
- 22 M. Lotya, Y. Hernandez, P. J. King, R. J. Smith, V. Nicolosi, L. S. Karlsson, F. M. Blighe, S. De, Z. Wang, I. T. McGovern, G. S. Duesberg and J. N. Coleman, *J. Am. Chem. Soc.*, 2009, **131**, 3611–3620.
- 23 L. Y. Xu, G. Y. Yang, H. Y. Jing, J. Wei and Y. D. Han, *Nanotechnology*, 2014, **25**, 055201.
- 24 B. Sun, B. Wang, D. W. Su, L. D. Xiao, H. Ahn and G. X. Wang, *Carbon*, 2012, **50**, 727–733.
- 25 C. Backes, K. R. Paton, D. Hanlon, S. Yuan, M. I. Katsnelson, J. Houston, R. J. Smith, D. McCloskey, J. F. Donegan and J. N. Coleman, *Nanoscale*, 2016, **8**, 4311–4323.
- 26 B. Wang, B. Luo, M. H. Liang, A. Wang, J. Wang, Y. Fang, Y. H. Chang and L. J. Zhi, *Nanoscale*, 2011, **3**, 5059–5066.
- 27 X. Zhang, A. C. Coleman, N. Katsonis, W. R. Browne, B. J. van Wees and B. L. Feringa, *Chem. Commun.*, 2010, **46**, 7539–7541.

- 28 G. Bepete, E. Anglaret, L. Ortolani, V. Morandi, K. Huang, A. Pénicaud and C. Drummond, *Nat. Chem.*, 2016, DOI: 10.1038/nchem.2669.
- 29 Y. Wei and Z. Sun, *Curr. Opin. Colloid Interface Sci.*, 2015, **20**, 311–321.
- 30 C. Backes, R. J. Smith, N. McEvoy, N. C. Berner, D. McCloskey, H. C. Nerl, A. O'Neill, P. J. King, T. Higgins, D. Hanlon, N. Scheuschner, J. Maultzsch, L. Houben, G. S. Duesberg, J. F. Donegan, V. Nicolosi and J. N. Coleman, *Nat. Commun.*, 2014, **5**, 4576.
- 31 X. Wang, L. Zhi and K. Muellen, *Nano Lett.*, 2008, **8**, 323–327.
- 32 M. W. Cao, N. N. Wang, L. Wang, Y. Zhang, Y. C. Chen, Z. L. Xie, Z. Y. Li, E. Pambou, R. H. Li, C. X. Chen, F. Pan, H. Xu, J. Penny, J. R. P. Webster and J. R. Lu, *J. Mater. Chem. B*, 2016, **4**, 152–161.
- 33 V. Nicolosi, M. Chhowalla, M. G. Kanatzidis, M. S. Strano and J. N. Coleman, *Science*, 2013, **340**, 1226419.
- 34 L. C. Cotet, M. Klara, M. Todea, M. C. Dudescu, V. Danciu and L. Baia, *J. Mater. Chem. A*, 2017, **5**, 2132–2142.
- 35 S. M. Notley, *Langmuir*, 2012, **28**, 14110–14113.
- 36 M. Lotya, P. J. King, U. Khan, S. De and J. N. Coleman, *ACS Nano*, 2010, **4**, 3155–3162.
- 37 U. Khan, A. O'Neill, M. Lotya, S. De and J. N. Coleman, *Small*, 2010, **6**, 864–871.
- 38 T. Skaltsas, N. Karousis, H.-J. Yan, C.-R. Wang, S. Pispas and N. Tagmatarchis, *J. Mater. Chem.*, 2012, **22**, 21507–21512.
- 39 A. C. Ferrari and D. M. Basko, *Nat. Nanotechnol.*, 2013, **8**, 235–246.
- 40 L. Niu, M. Li, X. Tao, Z. Xie, X. Zhou, A. P. Raju, R. J. Young and Z. Zheng, *Nanoscale*, 2013, **5**, 7202–7208.
- 41 S. H. Tamboli, B. S. Kim, G. Choi, H. Lee, D. Lee, U. M. Patil, J. Lim, S. B. Kulkarni, S. Chan Jun and H. H. Cho, *J. Mater. Chem. A*, 2014, **2**, 5077–5086.
- 42 W. Du, X. Jiang and L. Zhu, *J. Mater. Chem. A*, 2013, **1**, 10592–10606.
- 43 Y. Hernandez, V. Nicolosi, M. Lotya, F. M. Blighe, Z. Sun, S. De, I. McGovern, B. Holland, M. Byrne and Y. K. Gun'Ko, *Nat. Nanotechnol.*, 2008, **3**, 563–568.
- 44 W. Gao, L. B. Alemany, L. Ci and P. M. Ajayan, *Nat. Chem.*, 2009, **1**, 403–408.
- 45 D. Li, M. B. Müller, S. Gilje, R. B. Kaner and G. G. Wallace, *Nat. Nanotechnol.*, 2008, **3**, 101–105.

www.spm.com